

Monitoring water contamination in jet fuel using silica-based Bragg gratings

Christopher Holmes, Naruo Yoshikawa, Russell S. Minns, Greg Blanchard-Emmerson, Sam Watts, William S. Brocklesby, Jeremy G. Frey, Peter G.R. Smith

Abstract—This work quantifies water contamination in jet fuel (Jet A-1), using silica-based Bragg gratings. The optical sensor geometry exposes the evanescent optical field of a guided mode to enable refractometry. Quantitative analysis is made in addition to the observation of spectral features consistent with emulsification of water droplets and Stokes’ settling. Measurements are observed for cooling and heating cycles between ranges of 22°C and -60°C. The maximum spectral sensitivity for water contamination was 2.4 pm/ppm-v with a resolution of < 5 ppm-v.

Index Terms—Bragg gratings, Fuels, Integrated optics, Optical devices, Optical waveguides.

I. INTRODUCTION

THE hygroscopic nature of jet fuel means that over time water accumulates in the tank. If unmanaged this can form large quantities of hazardous ice due the large temperature decreases associated with high altitude flying, which can immobilize an aircraft’s engine. Whilst it is generally accepted by the industry that water accumulation in any form is undesirable, tolerable levels are considered to be no more than 90 parts per million by volume (ppm-v) for normal operation and 260 ppm-v for emergency operation [1,2]. In order to ensure these values are kept to a minimum, free (settled) water needs to be quantified and removed regularly. The current quantification procedure for onsite fuel quality control is a visual “clear/bright/transparency test”. Dissolved water cannot be seen with the naked eye but suspended water renders fuel dull, hazy, or cloudy in appearance [3]. The test is subjective rather than quantitative, sampling points are extremely limited, and monitoring is not continuous or conducted during flight.

This work considers quantification of water contamination in Jet A-1, using silica-based planar Bragg gratings. The technology could be developed to permit real-time distributed monitoring of the fuel system through use of an optical fibre network. If information can be acquired from such optical probes, then a better understanding of the fuel’s quality can be made. This can be used to ensure safety and potentially improve aircraft efficiency through effective fuel management. The technology has further advantages of being inherently safe in flammable environments, demonstrates an immunity to electromagnetic interference and can be spectrally multiplexed with other optical sensors [4].

Paper submitted on 19th November 2017. Work was sponsored by the Engineering and Physical Research Council (EPSRC), UK.

Authors’ are affiliated to the University of Southampton, UK. Dr Christopher Holmes, Dr. William Brocklesby and Prof Peter Smith are based in the Optoelectronics Research Centre and Dr Naruo Yoshikawa, Dr Russell Minns and Prof Jeremy Frey are based in the School of Chemistry. Dr Greg Blanchard-Emmerson and Dr Sam Watts have affiliation with Stratophase Ltd.

Dr Christopher Holmes is principal contact for this work (e-mail: christopher.holmes@southampton.ac.uk).

Studies concerning water contamination in jet fuel have been predominately made by the American and Russian military following early developments of the jet engine and high-altitude flight. Renewed interest in this area has recently emerged [1,2,5,6] due in part to the introduction of synthetic fuels such as synthetic paraffinic kerosene (SPK) and biokerosene, a drive to reduce an aircraft’s parasitic mass through effective water removal and recent incidents where ice formation has interfered with engine operation (highlighting fundamental limits in knowledge).

Optical technology is an ideal platform for probing jet fuel as typically there is no inherent spark risks. An optical fibre network can also be used to acquire distributed measurements through use of lightweight fibre interlinks, which only add a small amount of mass to the aircraft, compared to much heavier electronic cabling. This work utilizes Bragg gratings, which offer the ability for multi-parameter distributed monitoring through channel multiplexing in an optical network. It is noted that several recent publications have considered use of fibre Bragg gratings (FBGs) to monitor jet fuel, predominately using polymer based FBGs [5–7]. The reported polymer sensors operate via osmotic processes, where water ingresses into the polymer alters the optical properties of the medium. Through this approach, sensitivities of the order 60 pm/ppm (water content by mass) have been reported. The approach demonstrates high sensitivity, however it has an associated lag-time due to osmosis and does not discriminate against temperature fluctuations, factors that ultimately limit resolution. This work reports the probing of water contamination in jet fuel through evanescent field exposure in silica-based Bragg gratings. This is a real-time monitoring approach, which could be useful for fast flowing processes e.g. refuel or monitoring of engine feed lines. Further, the technology can temperature self-reference [4], an important feature in practice as large temperature fluctuations are known to exist during flight.

The presented refractometer, illustrated in Figure 1, is a commercial Stratophase Ranger Probe based upon silica planar technology. It is fabricated through small-spot direct UV writing, which simultaneously defines Bragg gratings and waveguides [4]. Evanescent field exposure of the guided mode is made through chemical wet-etching and enhanced by the deposition of a thin high-index overlayer [8]. The Bragg wavelength, λ_B , reflected from the grating is dependent upon the effective refractive index of the supported mode, n_{eff} , and the inherent period of the grating, Λ , related by:

$$\lambda_B = 2n_{eff}\Lambda \quad (1)$$

The sensor chip contains three Bragg gratings, separated spectrally

(through period) and spatially, shown in Figure 1. Bragg grating 1 (λ_1) and Bragg grating 2 (λ_2) are evanescently exposed. Sensitivity to external refractive index is enhanced for these gratings using a thin (10's of nanometers thick) titanium dioxide layer [4],[9]. Bragg grating 3 (λ_3) has a doped silica overlaid and is insensitive to external refractive index changes, meaning that it can be used as a thermal reference.

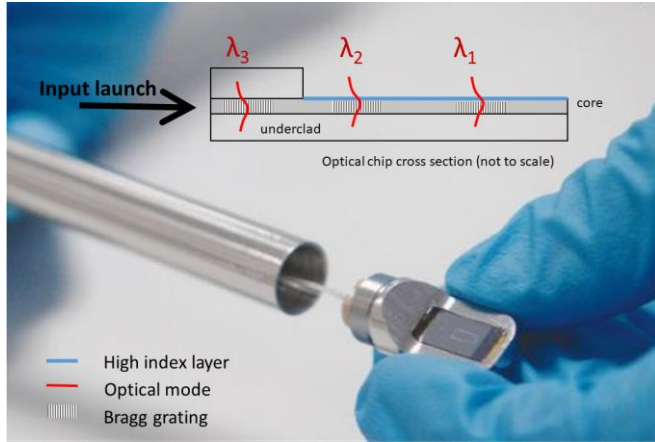


Fig. 1. The planar silica-on-silicon refractometer packaged in a stainless steel housing. Insert depicts layout of the optical chip, which contains three Bragg gratings (one buried with an overlaid λ_3 and the others exposed to the external environment).

II. METHODOLOGY AND RESULTS

Jet A-1 was sampled from Farnborough Airfield (January 2016). To achieve a 'dry fuel' baseline, a copulent amount of calcium hydride was added, stirred, set aside to settle and then removed through filtration.

The optical sensor chip was fiber-coupled, permitting interrogation of the reflection spectrum with a 3 dB coupler, polarization controller, ASE (Amplified Spontaneous Emission) light source and an Optical Spectrum Analyzer (OSA, Ando AQ6317B).

A. Spectral Response

Figure 2 illustrates the spectral response from the chip upon immersion into Jet A-1. The optical source is polarized and launched to have both transverse electric (TE) and transverse magnetic (TM) components. This is evident in the response of grating 3, which has both a TE and TM peak. Note, the birefringence of the waveguide is sufficiently large for both peaks to be resolvable. The increase in background noise above 1570 nm is a result of the limited bandwidth from the ASE source. Gratings 1 and 2 only have a TM peak in the presence of fuel as the orthogonal polarization (TE mode) is in a cut-off region. This has occurred as the commercial probe is designed to operate at a refractive index of 1.33, not that of jet fuel which is of the order 1.45. It should be noted that future work could optimize design to include both polarizations.

Figure 2 overlays two spectral scans for a dried fuel sample that has been temperature cycled. The data shows pre- and post-sonicated fuel. The thermal cycle took the fuel to below -50°C and returned it to room temperature through Newtonian heating. During cycling the fuel was open to the laboratory environment. It can be observed that after sonication the exposed gratings (gratings 1 and 2) blue shift and notably broaden in bandwidth. This is consistent with the formation of

an emulsion due to mechanical agitation. Here the free-standing water that is settled at the bottom of the fuel is emulsified, forming microscopic and ultra-microscopic water droplets (typically ranging from 0.1-100 μm) [10]. These suspended droplets act to reduce the average refractive index of the fuel. This changes the effective refractive index of the exposed optical mode, which linearly correlates to a blue shift in Bragg wavelength as outlined in Equation 1. Broadening in bandwidth is an indicator of inhomogeneity over the grating length, which would depend upon the size and distribution of the water droplets. In addition, Figure 2 shows an amplitude decrease for gratings 1 and 2, post sonication. This is consistent with spectral broadening. However, it should also be noted that the relative decrease in grating 1 is larger than that for grating 2. One explanation for this is increased scattering loss. Noting that light reflecting from grating 1 has a longer reflection path length (see Figure 1) and so a larger accumulated loss.

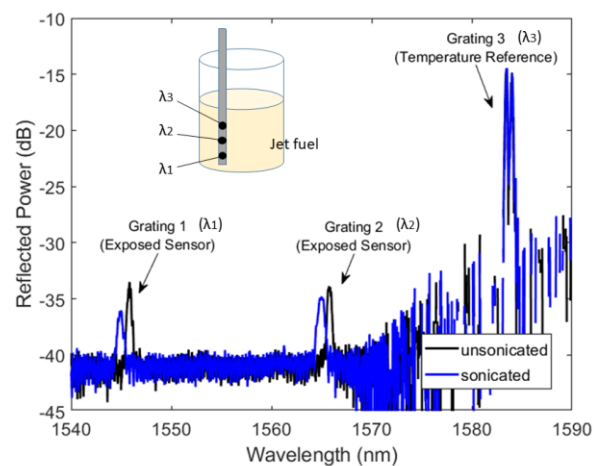


Fig. 2. The reflection spectrum from the sensor chip, showing three Bragg gratings in a sonicated and unsonicated jet fuel sample, measurement acquired at 22°C . Insert indicates arrangement of probe in the fuel.

The following section considers the effect of thermal cycling jet fuel, including the thermal cycle made for the data presented in Figure 2.

B. Thermo-Optic Response

Temperature variation experienced by jet fuel can, in extreme cases be less than -50°C . Understanding the characteristics of the fuel at these low temperatures is highly desirable for the aviation industry for enhanced safety and efficiency. This section makes some initial observations on thermal cycling of fuel. Thermal calibration was made through continuous spectral scanning and temperature monitoring using a PT1000 thermocouple. To interpret the parameters of the gratings (amplitude, bandwidth and central peak), the reflection spectra were fitted with Gaussian curves.

Figure 3 shows measured shifts in the central Bragg grating, for two different fuel samples, namely dried unsonicated and sonicated (previously illustrated in Figure 2, at 22°C). The thermal response of the exposed gratings (gratings 1 and 2) are almost an order of magnitude greater and of opposite sign to that of the buried grating (grating 3). This is understood to be a result of the high thermo-optic response of jet fuel and it having a comparably large refractive index [11]. The Bragg response for both exposed gratings is comparable, but the sensitivity of grating 2 seems marginally higher. This is partially a result of the larger grating period (see equation 1) and the fact that the

evanescent field penetration is greater at longer wavelengths, which acts to further enhance sensitivity. It is noted that the refractive index of Jet A-1 is similar to the sensor's glass substrate. As temperature decreases, the refractive index of the fuel increases and to a greater extent than the glass. This means that at sufficiently low temperature the TM mode is cut-off. This occurred below -12°C for dried jet fuel. It should be noted that whilst this limits the operational range of this particular sensor, future designs could be optimized (for example through altering the refractive index of the glass substrate or the enhancement layer), such to monitor dried fuel below -50°C .

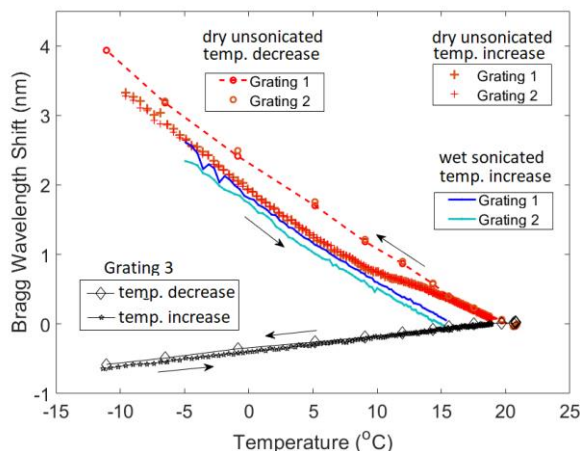


Fig. 3. The spectral response of the three Bragg gratings subject to a cool down and then warm up temperature cycle. The data includes a dried unsonicated sample and a wet sonicated sample. Arrows depict the direction of data acquisition. Spectral responses of exposed Bragg gratings are taken relative to the initial dried unsonicated sample.

From Figure 3, a hysteresis is seen to occur during temperature cycling of the dried unsonicated sample. Figure 4 examines this further through obviating any local temperature variation between the thermocouple and the chip. This is achieved by self-referencing the response of the exposed grating (grating 1 used here) to that of the buried grating (grating 3). The hysteresis is still present when represented in this form and thus considered a genuine feature. The time difference between each successive data point was approximately 10 seconds, meaning that the initial cooling process was approximately 1.5 minutes and the Newtonian heating made over a much larger timeframe. Deviation between the cool-down and warm-up sections occurs at approximately 15°C (note x-axis in Figure 4 is approximately linearly related to temperature). At 10°C there is a notable inflection, and a corresponding change in the thermo-optic response either side of this temperature (seen as a noticeable gradient change). The trend would suggest that the refractive index of the fuel is greater during fast cooling as opposed to a slow warming. An ingress of water into the fuel at low temperatures partially explains the spectral offset observed. It is understood that the fuel sample is exposed to ambient laboratory conditions, meaning there exists a water exchange rate between the air and fuel. Counterintuitively, continual warming of the fuel past 10°C actually reduces this offset until 16°C , at which point negligible deviation is observed. One postulation for this effect could be that water and ice droplets form in the fuel at low temperature. Above 10°C the water exchange rate decreases and the droplets fall under gravity in accordance with Stokes' Law. Previous work has quoted settling rates of the order $3\text{mm}\cdot\text{h}^{-1}$ [12], for 2-3 μm size diameter, with rate of settling scaling with the square of droplet radius. This theory would

suggest that the emulsion settles into free water and that there is negligible additional dissolved water added, as the spectral response returns to its pre-cooled value. This theory is corroborated through post-sonication of the sample (shown in Figure 2), which is consistent with the emulsification of free settled water. Interestingly, Figure 3 shows that after mechanical agitation the water droplets do not appear to settle in the same fashion as with the unsonicated test, when temperature-cycled once more. This may be due to droplet size, assuming that mechanical agitation forms much smaller water droplets, which in accordance with Stokes's Law take longer to settle.

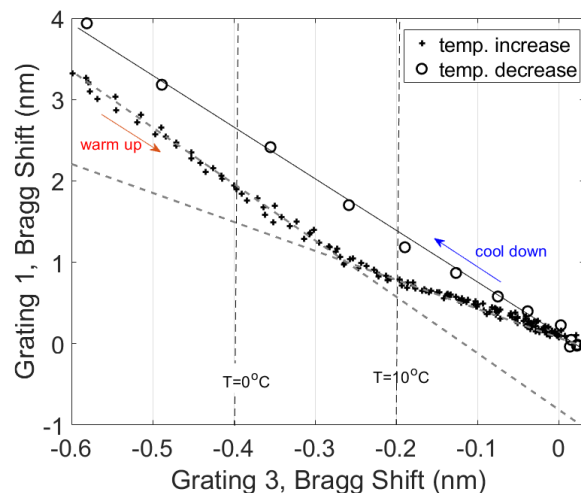


Fig. 4. The spectral response of grating 1, with respect to that of grating 3, upon warm up and cool down

Figure 5 shows the thermo-optic response (i.e. the spectral shift derivative with respect to temperature) for Bragg grating 1. The data presented includes Newtonian heating for a dried unsonicated sample and a 'known-to-be-wet' sonicated sample. The wet sample here is achieved through further addition and sonication of distilled water to the fuel. Water emulsion decreases the refractive index of the fuel and so the observed TM cut-off occurs at much lower temperatures. This means that the wet sample can be monitored at temperatures approaching -40°C .

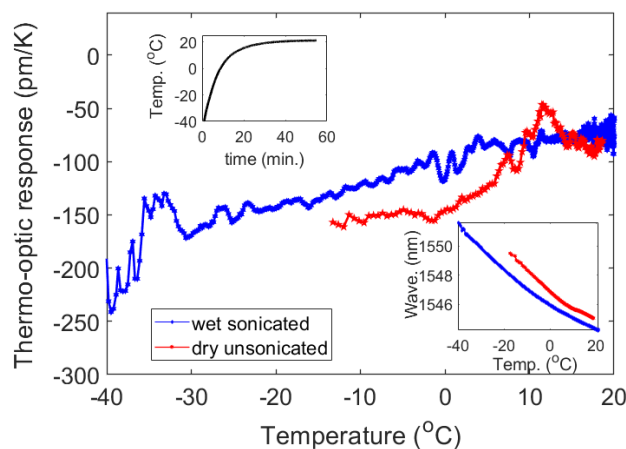


Fig. 5. Thermo-optic response from the sensor (inserts) depict the temperature data and spectral response from which main graph is calculated.

Dried fuel shows the smallest magnitude of thermo-optic response. This occurs at $\sim 11^{\circ}\text{C}$ and correlates to the inflection point previously

discussed. The thermo-optic response for the buried grating is 18 ± 3 pm/K, meaning that through exposure, the magnitude of the thermo-optic response can be enhanced by up to an order of magnitude. The small deviations observed in Figure 5 can be largely attributed to temperature differences between the thermocouple and sensor. There are two distinct features present in the wet sample that occur at 0°C and -33°C that correlate to changes in enthalpy.

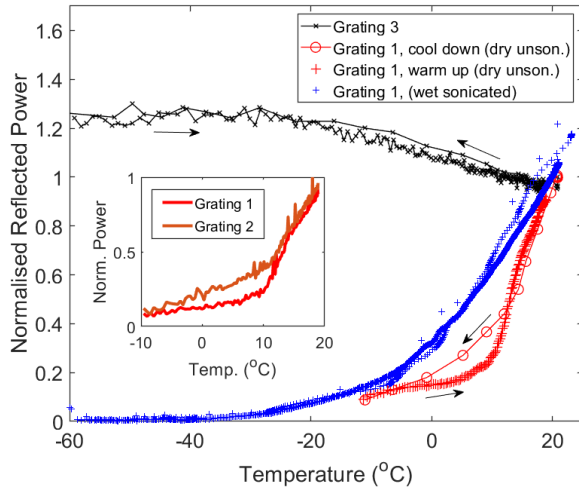


Fig. 6. Change in peak reflected power subject to cool down and warm up, arrows indicate the sequence of data. Insert, the cool down data for gratings 1 and 2 exposed to a dry unsonicated fuel sample. The data is normalized to the reflection amplitude at room temperature.

Information about fuel can be additionally concluded from the amplitude and bandwidth response of the gratings. Figure 6 illustrates the normalized peak reflectivity (i.e. the grating amplitude) as a function of temperature. The buried temperature reference grating (grating 3) increases in amplitude as temperature decreases. This is largely due to a reduction in the noise floor, attributed to reduced broadband scattering in the exposed region. The peak reflectivity for both of the exposed gratings (gratings 2 and 3) decrease with temperature. This behavior is largely expected as modal power shifts from the core of waveguide to the fuel causing model mismatch between the buried and exposed transition. Data for the dried fuel sample again shows a unique inflection feature, centered $\sim 10^\circ\text{C}$. This is only present for the Newtonian heating and so consistent with the hysteresis artifact previously discussed. Similarly, hysteresis is not observed for the wet sonicated samples. It is noted that water droplets would additionally result in scattering losses and so a contribution to the reduction in reflected power. Note, the fractional reduction in peak reflected power is larger for grating 1 than for grating 2 (see Figure 6 insert). This is a marker of increasing propagation loss, consistent with scattering mechanisms such as those induced by suspended water droplets.

Figure 7 illustrates the variation in spectral bandwidth as a function of temperature. The raw spectral data has a 2 pm resolution and bandwidth was deduced through use of a Gaussian fitting algorithm. Large associated errors exist with the fit, however, distinct trends can still be observed. The general trend is that a sonicated sample has a broader bandwidth than an unsonicated sample, consistent with inhomogeneity in the fuel. For the dried fuel sample bandwidth decreases with increasing temperature, which is consistent with settling of larger water droplets previously postulated, i.e.

removal of inhomogeneity (water emulsion).

Optical responses considered so far have not been quantitatively measured. The following section therefore presents quantified analysis for water in sonicated fuel.

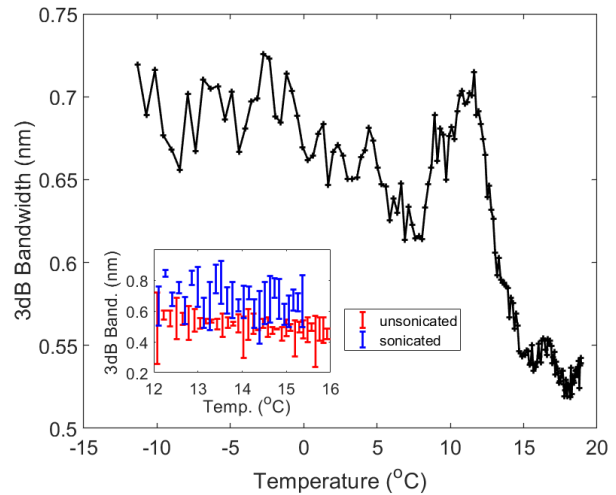


Fig. 7. Grating 1 bandwidth response for a dry unsonicated sample subject to temperature increase. Insert depicts averaged bandwidth data for grating 1 and grating 2 upon warm up.

C. Quantitative Water Contamination

Water contaminated samples were prepared through the addition of deionized water to a 100 mL of dried Jet A-1. The approach consecutively added volumes of 5 μL , 15 μL , 35 μL , 85 μL and 135 μL . Between each increment the sample was sonicated and optically measured. Figure 8 presents the spectral response of all three Bragg gratings. Each data point is averaged from ten scans and the data from all three gratings taken to produce a thermally compensated shift. Compensation is made from calibrated thermo-optic responses. It can be observed that increasing water contamination reduces the Bragg response. This follows a nonlinear trend, characteristic of evanescent field sensitivity [11]. The region of most interest for aviation is at contamination levels < 90 ppm-v. This is the region where maximum sensitivity is observed, equating to 2.4 pm/ppm-v.

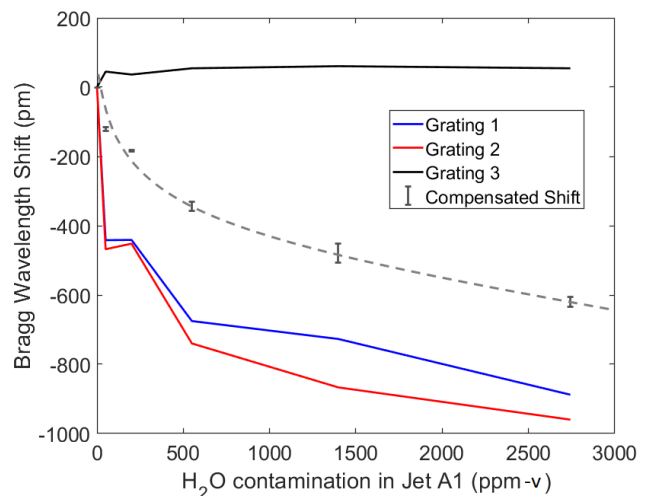


Fig. 8. The Bragg wavelength shift as a function of water contamination. Data compensation correlated with temperature.

Peak reflected power from the exposed Bragg gratings, are

illustrated in Figure 9. The plot takes the averaged peak amplitude (from gratings 1 and 2) and temperature compensates by 0.4 dB/K, which is estimated from the data presented in Figure 6. The insert in Figure 9 shows the raw data from which the main plot is derived. The general trend observed is that for increasing levels of water contamination there is a decrease in grating amplitude. It can be further observed that the relative difference between two separate gratings (in decibels) is approximately equal. This suggests that there is a negligible measurable increase in propagation loss (i.e. scattering from the suspended water) for increasing levels of water contamination. It is noted that for the unique case of 0 ppm-v propagation losses are significantly different, which can largely be attributed to scattering from suspended water droplets. The overall trend for loss is considered to largely be a function of modal mismatch, brought about through refractive index variation in the fuel samples. This response could be minimized in future designs through an adiabatic change between the different modes. Through use of an adiabatic transition and adoption of multi-grating regression [13], smaller changes in propagation loss could be extracted. This could be used to infer water droplet sizes and density.

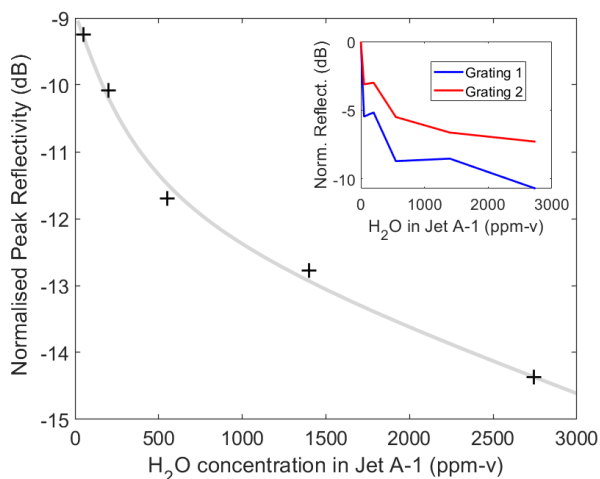


Fig. 9. Temperature compensated reflected power as a function of water contamination in Jet A-1 (insert) is the raw data from grating 1 and 2.

III. DISCUSSION

This work highlights the potential in using silica-based evanescent field sensors to detect water contamination in jet fuel. The work demonstrates a resolution of the order 5 ppm-v within the operational water contamination range for jet A-1, namely <90 ppm-v. Further, it has been shown that information about suspended water droplets in the fuel could be inferred through observing scattering properties and inhomogeneity, evident through changes in relative grating amplitude and bandwidth. Forming such an understanding of suspended water is important as it could be used to deduce settling times required for effective water capture. That is to say, to inform a decision on the length of time required for a plane to be taken out of service in order to extract an 'optimal' quantity of water.

As far as the authors are aware, this work demonstrates the largest thermal sensitivity enhancement observed for silica waveguides. This is interesting, for a host of applications, including optically integrated quantum technology, where thermo-optic phase shifters are used for entangled photon experiments [14]. As circuit complexity scales

thermal management becomes more challenging. Leveraging an order of magnitude in thermal response could significantly reduce the Ohmic heating of such chips. Through enhanced thermal sensitivity, it should be possible to improve the thermo-optic tuning of planar Bragg gratings from current limits of around 150 GHz in the C-band [15-16], to around 1 THz. As polymers have a large thermal expansion coefficient, record values of thermal sensitivity for silica FBGs have been achieved through embedding into polymer materials such as Teflon, PMMA PLA and TPU [17-19]. These have provided sensitivities of up to 150 pm/K (at 300K) [18]. The values observed in this work exceed these and furthermore are not prone to delamination or creep.

Waveguide losses observed in this work are largely considered to be a result of modal mismatch as light propagates from the buried to the etched region. This could be reduced through forming an adiabatic taper between the sections. Such a feature should act to maximize signal to noise, enhance range and sensitivity.

IV. CONCLUSION

The use of silica-based optical Bragg sensors to detect water contamination in jet fuel has been demonstrated. The sensors used enhanced evanescent fields to probe the fuel and attain levels of contamination below 5 ppm-v. It should be noted that the specific commercial sensor used is designed for operation at refractive indices about 1.33 not that of jet fuel which is of the order 1.45. The technology and geometry of the sensor chip can in future work be adapted to further increase sensitivity and the operational range of the device.

Through monitoring grating bandwidth and relative amplitudes, it was inferred that information about suspended water droplets can be deduced. Such information can be utilized for distributed monitoring and to map and understand phenomena in large fuel systems, which would contribute to more efficient fuel management.

A record level of thermal sensitivity for the silica-based Bragg grating was observed. The thermo-optic response of the Bragg gratings at a 243 K was 18 ± 3 pm/K. The exposed gratings enhanced this by an order of magnitude 170 ± 1 pm/K. As a result of the large thermo-optic response of the sensor when exposed to fuel, it is imperative for local thermal compensation, achieved in this work using a localized buried Brag grating.

REFERENCES

- [1] SAE-International, AIR790 considerations on ice formation in aircraft fuel systems. Technical report. Ae-5 Aerospace Fuel, Oil And Oxidizer Systems Committee; 2006.
- [2] SAE-International, AIR1401 aircraft fuel system and component icing test. Technical report. Ae-5 Aerospace Fuel, Oil And Oxidizer Systems Committee; 2007.
- [3] J. Hemighaus, G. Boval, T. Bacha, J. Barnes, F. Franklin, M. Gibbs, L. Hogue, N. Jones, J. Lesnini, D. Lind, J. Morris, "Aviation Fuels Technical Review," 2006.
- [4] C. Holmes, J. C. Gates, L. G. Carpenter, H. L. Rogers, R. M. Parker, P. A. Cooper, S. Chaotan, F. R. M. Adikan, C. B. E. Gawith, and P. G. R. Smith, "Direct UV-written planar Bragg grating sensors," *Meas. Sci. Technol.*, vol. 26, no. 11, pp. 112001, 2015.

- [5] S. Baena-Zambrana, S.L. Repetto, C.P. Lawson, J.K.-W. Lam, 'Behaviour of water in jet fuel – A literature review', *Progress in Aerospace Sciences* 60 pp. 35-44, 2013.
- [6] J.K.-W. Lam, J.I. Hetherington, M.D. Carpenter, 'Ice growth in aviation jet fuel', *Fuel*, vol. 113, pp.402-406, 2013.
- [5] C. Zhang, X. Chen, D. J. Webb, and G.-D. Peng, "Water detection in jet fuel using a polymer optical fibre Bragg grating," in *20th International Conference on Optical Fibre Sensors*, vol. 750380, no. October 2009, p. 750380, 2009.
- [6] W. Zhang, D. J. Webb, M. Carpenter, and C. Williams, "Measuring water activity of aviation fuel using a polymer optical fiber Bragg grating," *Proc. of SPIE*, vol. 9157, p. 91574V, 2014.
- [7] D. J. Webb, "Fibre Bragg grating sensors in polymer optical fibres," *Meas. Sci. Technol.*, vol. 26, no. 9, pp. 1–11, 2015.
- [8] G. R. Quigley, R. D. Harris, and J. S. Wilkinson, "Sensitivity enhancement of integrated optical sensors by use of thin high-index films", *Appl. Opt.*, vol. 38, no. 28, pp. 6036–9, 1999.
- [9] I. J. G. Sparrow, P. G. R. Smith, G. D. Emmerson, S. P. Watts, and C. Riziotis, "Planar Bragg Grating Sensors—Fabrication and Applications: A Review," *J. Sensors*, vol. 2009, pp. 1–12, 2009.
- [10] S. Baena-Zambrana, S.L. Repetto, C.P. Lawson, J.K.-W. Lam, 'Behaviour of water in jet fuel – A literature review', *Progress in Aerospace Sciences* 60 pp. 35-44, 2013.
- [11] R. C. Kamikawachi, I. Abe, H. J. Kalinowski, J. L. Fabris, and J. L. Pinto, "Nonlinear temperature dependence of etched fiber bragg gratings," *IEEE Sens. J.*, vol. 7, no. 9, pp. 1358–1359, 2007.
- [12] J.K.-W. Lam, J.I. Hetherington, M.D. Carpenter, "Ice growth in aviation jet fuel", *Fuel*, vol. 113, pp.402-406, 2013
- [13] A. C. Gray, A. Jantzen, P. C. Gow, D. H. Smith, C. B. E. Gawith, P. G. R. Smith, and C. Holmes, "Leaky mode integrated optical fibre refractometer", *Optics Express*, vol. 26, no. 7, pp. 9155-9164, 2018
- [14] J. B. Spring, B. J. Metcalf, P. C. Humphreys, W. S. Kolthammer, X.-M. Jin, M. Barbieri, A. Datta, N. Thomas-Peter, N. K. Langford, D. Kundys, J. C. Gates, B. J. Smith, P. G. R. Smith, and I. A. Walmsley, "Boson Sampling on a Photonic Chip," vol. 50502, no. February, pp. 798–802, 2012.
- [15] C. Holmes, D. O. Kundys, J. C. Gates, C. B. E. Gawith, and P. G. R. Smith, "150 GHz of thermo-optic tuning in direct UV written silica-on-silicon planar Bragg grating," *Electron. Lett.*, vol. 45, no. 18, p. 954, 2009.
- [16] P. A. Cooper, L. G. Carpenter, C. Holmes, C. Sima, J. C. Gates, and P. G. R. Smith, "Power-Efficiency Enhanced Thermally Tunable Bragg Grating for Silica-on-Silicon Photonics," *IEEE Photonics J.*, vol. 7, no. 2, pp. 1–11, 2015.
- [17] V. Mishra, M. Lohar, and A. Amphawan, "Improvement in temperature sensitivity of FBG by coating of different materials," *Optik (Stuttg.)*, vol. 127, no. 2, pp. 825–828, 2016.
- [18] T. Mizunami, H. Tatehata, and H. Kawashima, "High-sensitivity cryogenic fibre-Bragg-grating temperature sensors using Teflon substrates," *Meas. Sci. Technol.*, vol. 12, no. 7, p. 914, 2001.
- [19] A. Leal-Junior, J. Casas, C. Marques, M. Pontes, and A. Frizera, "Application of Additive Layer Manufacturing Technique on the Development of High Sensitive Fiber Bragg Grating Temperature Sensors," *Sensors*, vol. 18, no. 12, p. 4120, 2018.